used for mobile robot localization is called Monte Carlo Localization (MCL), and this modified version is called MCL with planned sampling [16] or Mixture MCL [18].

In the prediction phase, the SIR Particle filter samples from the importance density $p\left(\mathbf{x}_k \left| \mathbf{x}_{k-1}^{(i)}, \mathbf{u}_{k-1} \right.\right)$, which does not depend on the last observation. So, the samples are predicted from the motion model, and then the most recent observation is used to adjust the importance weights of this prediction. The idea used in this enhancement to particle filtering is to add to those samples predicted from the motion model some samples predicted from the most recent observation [18]. The importance weights of these new samples are adjusted according to the probability samples of the last iteration and the latest vehicle motion. These new samples are called planned samples [16] or samples generated from the dual of MCL [18].

The planned samples are drawn from the importance density $p\left(\mathbf{z}_k \left| \mathbf{x}_k \right.\right)$ which is the observation likelihood. These samples are consistent with the most recent observation but ignorant of the previous belief about the vehicle state $p\left(\mathbf{x}_{k-1} \left| Z_{k-1} \right.\right)$ and the motion $\mathbf{u}_{k-1}$. The samples are weighted using $p\left(\mathbf{x}_k^{(i)} \left| \mathbf{x}_{k-1}^{(i)}, \mathbf{u}_{k-1} \right.\right)$. The version of PF that uses this type of sampling alone is known as likelihood PF [19].

In the version of PF used in this research and as described in [18], a number of samples (a suitably chosen ratio from the total number of samples) are drawn from $p\left(\mathbf{z}_k \left| \mathbf{x}_k \right.\right)$ and added to the samples drawn from $p\left(\mathbf{x}_k \left| \mathbf{x}_{k-1}^{(i)}, \mathbf{u}_{k-1} \right.\right)$. Samples in these two groups are weighted with their respective weight update equations, and then the resampling is achieved. According to [18], these two importance densities have complimentary advantages and disadvantages, so their combination gives better performance. This version of PF will be called Mixture Particle filter after the name used in [18], because it samples from a mixture of importance densities. Mixture PF also enables the use of a much smaller number of samples as compared to SIR PF.

4 PARALLEL CASCADE IDENTIFICATION

System identification is an effort to infer the dynamic characteristics between system input and output from an analysis of time-varying input-output data. Most of the techniques assume linearity due to the simplicity of analysis as nonlinear techniques make analysis much more complicated and difficult than for the linear case. However, for more realistic dynamic characterization, nonlinear techniques are suggested. Parallel cascade identification (PCI) is a nonlinear system identification technique proposed by M.J. Korenberg [20]. This technique models the input/output behavior of a nonlinear system by a sum of parallel cascades of alternating dynamic linear (L) and static nonlinear (N) elements. The parallel array can be built up one cascade at a time [21].

Palm [22] proved that any discrete-time Volterra series with finite memory and anticipation can be uniformly approximated by a finite sum of parallel LNL cascades, where the static nonlinearities N are exponentials and logarithmic functions. Korenberg [21] showed that any discrete-time doubly finite (finite memory and order) Volterra series can be exactly represented by a finite sum of LN cascades where the N are polynomials. A key advantage of this technique is that it is not dependent on a white or Gaussian input, but the identified individual L and N elements may vary depending on the statistical properties of the input chosen [21]. The cascades can be found one at a time and nonlinearities in the models are localized in static functions. This reduces the computation as higher order nonlinearities are approximated using higher degree polynomials in the cascades rather than higher order kernels in a Volterra series approximation.

The method begins by approximating the nonlinear system by a first such cascade. The residual (i.e., the difference between the system and the cascade outputs) is treated as the output of a new nonlinear system, and a second cascade is found to approximate the latter system, and thus the parallel array can be built up one cascade at a time. Let $y_k(n)$ be the residual after fitting the k-th cascade, so $y_o(n) = y(n)$. Let $z_k(n)$ be the output of the k-th cascade, so

$$y_k(n) = y_{k-1}(n) \quad - \quad z_k(n) \ \textit{where } k=1,2,\ldots. \tag{5}$$

The dynamic linear elements in the cascades can be determined in a number of ways [21, 23]. The method employed in this paper uses cross correlations of the input with the current residual. Best fitting of current residual were used to find the polynomial coefficients of the static nonlinearities. These resulting cascades are such as to drive the cross correlations of the input with the residual to zero [21, 23]. However, a few basic parameters have to be specified in order to identify a parallel cascade model, as follows:

(1) The memory length of the dynamic linear element that begins each cascade: this can be seen from the following equation

$$u_k(n) = \sum_{j=0}^{R} g_k(j)x(n-j) \tag{6}$$

where the linear element's output $u_k(n)$ depends on input values $x(j)$, $x(j\text{-}1)$, ... $x(j\text{-}R)$ so its memory length is $R+1$, *and* $g_k(j)$, is the impulse response of the linear element.

(2) The degree D of the polynomial static nonlinearity

that follows the linear element: this polynomial is best fit to minimize the MSE of the approximation of the residual.

(3) The maximum number of cascades allowable in the model;

(4) A threshold based on a standard correlation test for determining whether a cascade's reduction of the mean-square error (MSE) justifies its addition to the model.

$$\overline{z_k^2(n)} > \frac{4}{T-R+1}\overline{y_{k-1}^2(n)} \tag{7}$$

In Equations (10), $\overline{z_k^2(n)}$ denotes the mean square of the candidate cascade's output, and $\overline{y_{k-1}^2(n)}$ denotes the mean square of the current residual, i.e., the residual remaining from the cascades already present in the model.

5 NONLINEAR MODELS FOR TIGHTLY COUPLED INTEGRATION

In tightly coupled RISS/GPS system architecture instead of using the position and velocity solution from the GPS receiver as input for the fusion algorithm, raw GPS observations such as pseudoranges and Doppler shifts are used. The range measurement is usually known as a pseudorange due to the contamination of errors as well as synchronization errors between the satellite and receiver clocks. The pseudorange measurement for the m^{th} satellite can be written as [2,3].

$$\rho^m = r^m + c\delta t_r - c\delta t_s + cI^m + cT^m + \varepsilon_\rho^m \tag{8}$$

where ρ^m: is the m^{th} satellite to receiver measured pseudorange (meters), r^m: the true range between m^{th} satellite and receiver (meters), c: speed of light (meters/second), δt_r: receiver clock bias (second), δt_s: satellite clock bias (second), I^m: ionospheric delay from m^{th} satellite (second), T^m: tropospheric delay from m^{th} satellite (second), ε_ρ^m: error in range mainly due to receiver noise (meters).

After compensating for satellite clock bias, Ionospheric and Tropospheric errors, we can write the corrected pseudorange as [2],

$$\rho_c^m = r^m + c\delta t_r + \tilde{\varepsilon}_\rho^m \tag{9}$$

where $\tilde{\varepsilon}_\rho^m$ is the total effect of residual errors.

The geometric range from m^{th} satellite to receiver is

$$\begin{aligned} r^m &= \sqrt{(x-x^m)^2 + (y-y^m)^2 + (z-z^m)^2} \\ &= \left\| \mathbf{x} - \mathbf{x}^m \right\| \end{aligned} \tag{10}$$

where $\mathbf{x} = [x, y, z]^T$ is the receiver position in ECEF frame, and $\mathbf{x}^m = [x^m, y^m, z^m]^T$ is the position of the m^{th} satellite in ECEF frame

In vector form, equation (9) can be written as:

$$\rho_c^m = \left\| \mathbf{x} - \mathbf{x}^m \right\| + b_r + \tilde{\varepsilon}_\rho^m \tag{11}$$

where $b_r = c\delta t_r$ is the error in range (in meters) due to receiver clock bias. This equation is nonlinear, the traditional techniques relying on KF used to linearize these equations about the pseudorange estimate got from the inertial sensors mechanization, and the details of this operation are described in [24]. Since PF is used in this paper and it can accommodate nonlinear models, there is no need for linearizing this equation [25].

The receiver clock error and the residual errors assumed as white Gaussian noise are the only errors modeled inside the measurement model in the tightly-coupled solutions presented in the literature. Experimental investigation of the GPS pseudoranges in trajectories in different areas and scenarios showed that the residual errors are not just white noise as assumed in the literature, but they are correlated errors. As the GPS observables are used to update the PF, a technique must be developed to adequately model these errors to improve the overall performance of PF. This research proposes using PCI to model these correlated errors. The PCI module models these errors, and then provides correction prior to sending the GPS pseudoranges to aid PF during periods of GPS partial outages.

6 AUGMENTED PF-PCI FOR INTEGRATED RISS/GPS

In section 4, the parallel cascade model was briefly presented, together with a simple method for building up the model to approximate the behavior of a dynamic nonlinear system, given only its input and output. In order to apply PCI to 3D RISS /GPS integration, this paper proposes an M-PF-PCI module where the role of PCI is to model the residual errors of GPS pseudoranges.

In full GPS coverage when 4 or more satellites are available to the GPS receiver, the PF integrated solution provides adequate position benefiting from both GPS and RISS readings, and the PCI builds the model for the pseudoranges errors for each visible satellite. The input of each PCI module is the pseudorange of the visible mth GPS satellite (ρ_{GPS}^m), and the reference output $\Delta\rho_R^m$ is the difference of GPS observed pseudorange ($\Delta\rho_R^m$) compared with of the estimated mth pseudorange from the corrected navigation solution ($\rho_{Nav-Sol}^m$) to derive the residual error of pseudorange as given in Equation (12).

$$\Delta\rho_R^m = \rho_{Nav-Sol}^m - \rho_{GPS}^m \tag{12}$$

The reference output $\Delta\rho_R^m$ does not apply any correction during full GPS coverage. It is only used as a reference output to build the PCI model. Dynamic characteristics between system input and output help to achieve a residual pseudorange error model.

During partial GPS coverage, when there are less than 4 satellites available, the PCI modules for all satellites cease training, and the available PCI model for each visible satellite will be used to predict the corresponding residual pseudorange errors. The PF operates as usual, but in this instance, the GPS observed pseudorange is corrected by the output of the corresponding PCI. The pre-built PCI models only for the visible satellites during the partial outage predict the corresponding residual pseudorange errors $\Delta\rho_R^m$ to obtain a correction. Thus, the corrected pseudorange $\rho_{Corrected}^m$ can then be obtained as given in Equation (12):

$$\rho_{Corrected}^m = \rho_{GPS}^m - \Delta\rho_R^m \tag{13}$$

During a full GPS outage, when no satellites are available, PF operates in prediction mode and the PCI modules neither provide correction nor operate in training modes.

7 EXPERIMENTAL SET UP

The performance of the developed navigation solution was examined with road test experiments in a land vehicle. The experimental data collection was carried out using a full size passenger van carrying a suite of measurement equipment that included inertial sensors, GPS receivers, antennae, and computers to control the instruments and acquire the data The inertial sensors used in this work are from the MEMS-grade IMU made by Crossbow whose model is IMU300CC-100. The specifications of this IMU are in Table 1, and the detailed specifications can be found in [26].

The vehicle's forward speed readings were obtained through vehicle built-in sensors via the on-board diagnostics version II (OBD-II) interface using a device called CarChip. The specifications of this device are described in [27], and more details about OBD-II speed readings can be found in [28]. The sample rate for the collection of speed readings was 1 Hz. To demonstrate the performance of the proposed solution GPS receiver used was the NovAtel OEMV-1G [29]. The results were evaluated with respect to a reference solution made by NovAtel, where Honeywell HG1700 tactical grade IMU [30] was integrated with the NovAtel OEM4 GPS receiver[31]. Together the NovAtel and Honeywell systems were integrated with an off-the-shelf unit developed by NovAtel, the G2 Pro-Pack SPAN unit [32]. The NovAtel system provided the reference solution to validate the proposed method and to examine the overall performance during simulated GPS outages.

Table 1: Crossbow IMU specifications [26].

Accelerometer	
Range	± 2 g
Bias	± 30 mg
Scale Factor	< 1 %
Random Walk	< 0.15 m/s/ $\sqrt{hr}$
Gyroscope	
Range	± 1000 deg/sec
Bias	< ± 2.0 deg/sec
Scale Factor	< 1 %
Random Walk	< 2.25 deg / $\sqrt{hr}$
Linearity	< 1%

8 EXPERIMENTAL RESULTS

Several road test trajectories were carried out using the setup described above. The road test trajectory considered for this paper was performed from Toronto to Kingston, Ontario, Canada as shown.in the Figure 1

Figure 1: Track of the trajectory conducted from Toronto to Kingston, ON, Canada. Circles indicate the locations of GPS outage.

This road test was performed for nearly 140 minutes of continuous vehicle navigation and a distance of around 230 km. Six simulated GPS outages of 60-second each were introduced in post-processing (they are shown as blue circles overlaid on the map in (Figure 1)) during good GPS availability. The trajectory was run four times with the simulated partial outages having 3, 2, 1, and 0 visible satellites, respectively. The errors estimated by PF-PCI, PF-only, KF-PCI and KF-only solutions were evaluated with respect to the NovAtel reference solution.

The results in Figure 2 demonstrate the benefits of the proposed M-PF-PCI module to model the pseudorange errors. The main benefit of using PCI for pseudorange correction is the modeling capabilities of PCI, which enabled correction of the raw GPS measurements. The benefit of having more satellites available can also be seen from these results. The general trend is that having three satellites visible is better than two, which is better than the one and zero cases.

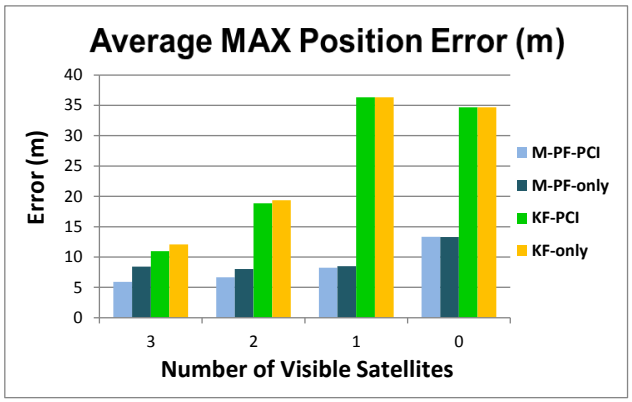

Figure 2: Bar graph showing average maximum positional errors for all partial GPS outages.

9 CONCLUSION

The work presented in this paper shows the performance of a novel design that has been implemented using PCI to model the pseudorange errors in the M-PF measurement model of a tightly coupled PF system for integrating low-cost MEMS-based 3D RISS and GPS observations to produce an integrated positioning solution. A PCI module is built for each satellite during good availability where the integrated solution presents a very good position estimate. Then each PCI module output provides pseudorange corrections to the GPS pseudorange of the corresponding visible satellite during GPS partial outages, thereby decreasing residual errors in the GPS observation. This PCI-PF module has been tested with real road-test trajectories and compared to M-PF-only, KF-PCI, KF-only for tightly coupled 3D RISS/GPS integrated solutions. The results for one trajectory with six simulated 60-second GPS partial outages have been presented. PCI-PF module has been able to improve the overall maximum position error during the GPS partial outages.

10 ACKNOWLEDGEMENTS

This research was supported in part by research grants from Natural Sciences and Engineering Research Council (NSERC), Geomatics for Informed Decision (GEOIDE) Network Centers of Excellence, and Defence Research and Development Canada (DRDC) Ottawa. The equipment was acquired by research funds from Canada Foundation for Innovation, Ontario Innovation Trust and the Royal Military College of Canada.

REFERENCES

[1] El-Rabbany, *Introduction to GPS -The Global Positioning System*. Norwood: Artech House Inc., 2002.

[2] P. Misra and P. Enge, *Global Positioning System: Signals, Measurements and Performance*: Ganga-Jamuna P, Dec 2001.

[3] E. D. Kaplan and C. J. Hegarty, *Understanding GPS Principles and Applications*, 2nd ed. Norwood: Artech House, Inc., 2006.

[4] J. A. Farrell, *Aided Navigation: GPS with High Rate Sensors*: McGraw-Hill Professional, Mar 2008.

[5] M. S. Grewal, L. R. Weill, and A. P. Andrews, *Global Positioning Systems, Inertial Navigation, and Integration*, 2nd ed., New Jersey: Wiley-Interscience, 2007.

[6] A. Noureldin, T.B. Karamat, M. D. Eberts, A. El-Shafie, "Performance Enhancement of MEMS Based INS/GPS Integration for Low Cost Navigation Applications," *IEEE Transactions on Vehicular Technology*, vol. 58, no. 3, pp. 1077-1096, March 2009.

[7] J. Georgy, A. Noureldin, M. Korenberg, and M. Bayoumi, "Low Cost Three Dimensional Navigation Solution for RISS/GPS Integration Using Mixture Particle Filter," *IEEE Transactions on Vehicular Technology*, vol. 59, no. 2, pp. 599-615, February 2010.

[8] T. B. Karamat, J. Georgy, U. Iqbal, and A. Noureldin, "A Tightly-Coupled Reduced Multi-Sensor System for Urban Navigation", in *Proceedings of ION GNSS 2009*, Savannah, Georgia, USA, September 2009.

[9] U. Iqbal and A. Noureldin, "*Integrated Reduced Inertial Sensor System/GPS for Vehicle Navigation*," VDM Verlag, 2009

[10] U. Iqbal, A. F. Okou, and A. Noureldin, "An integrated reduced inertial sensor system - RISS/GPS for land vehicle", *in Proceedings of IEEE/ION*

PLANS 2008, pp.912-922, Monterey, California, USA, May 2008.

[11] J. Georgy, U. Iqbal, M. Bayoumi, A, Noureldin, "Reduced Inertial Sensor System (RISS)/GPS Integration Using Particle Filtering for Land Vehicles" in *Proceedings of the 21st International Technical Meeting of the Satellite Division of the Institute of Navigation (ION GNSS 2008)*, Savannah, GA, USA, 16–19 September 2008; pp. 30-37.

[12] A. Doucet, S.J. Godsill, and C. Andrieu, "On sequential monte carlo sampling methods for bayesian filtering," *Statistics and Computing*, vol. 10, pp. 197–208, November 2000.

[13] H.L. Dyckman, S. Sloat, and B. Pettus, "Particle filtering to improve GPS/INS integration", in *Proceedings of the International Technical Meeting of the Satellite Division of the Institute of Navigation (ION GNSS 2004)*, pp. 1619-1626, Long Beach, CA, USA , September 2004.

[14] N.J. Gordon, D.J. Salmond, and A.F.M. Smith, "Novel approach to nonlinear/nongaussian bayesian state estimation," in *IEE Proceedings -F (Radar and Signal Processing)*, vol. 140, pp. 107–113, 1993.

[15] F. Dellaert, D. Fox, W. Burgard, and S. Thrun, "Monte carlo localization for mobile robots," in *Proceedings of IEEE ICRA-99*, Detroit, MI, USA, 1999.

[16] P. Jensfelt, "Approaches to Mobile Robot Localization in Indoor Environments", *Ph.D. thesis*, Department of Sensors, signals and systems, Royal Institute of Technology, Sweden, 2001.

[17] P. Jensfelt, O. Wijk, D. Austin, and M. Andersson, "Experiments on augmenting condensation for mobile robot localization," in *Proceedings. of IEEE ICRA-2000*, vol. 3, pp. 2518–2524, San Francisco, CA, USA, 2000.

[18] S. Thrun, D. Fox, W. Burgard, and F. Dellaert, "Robust monte carlo localization for mobile robots," *Artificial Intelligence*, vol. 128, pp. 99–141, 2001.

[19] M. S. Arulampalam, S. Maskell, N. Gordon, and T. Clapp, "A tutorial on particle filters for online nonlinear/non-gaussian bayesian tracking", *IEEE Transactions on Signal Processing*, vol. 50, no. 2, February 2002.

[20] M. J. Korenberg, Statistical identification of parallel cascades of linear and nonlinear systems. *Sixth IFAC Symposium on Identification and System Parameter Estimation*, 1982, Vol. 1, pp. 580–585.

[21] M. J. Korenberg, "Parallel cascade identification and kernel estimation for nonlinear systems", *Annals of Biomedical Engineering*, Vol. 19, pp. 429-455, 1991.

[22] G. Palm, "On Representation and Approximation of Nonlinear Systems. Part II: Discrete Time." *Biological Cybernetics*, Vol. 34, pp 49-52, 1979.

[23] J. M. Eklund, and M. J. Korenberg, "Simulation of Aircraft Pilot Flight Controls Using Nonlinear System Identification", *Simulation*, Vol. 75, No. 2, pp.72-81, 2000.

[24] T. B. Karamat, "Implementation of Tightly Coupled INS/GPS Integration for Land Vehicle Navigation", *M.Sc. Thesis*, Department of Electrical and Computer Engineering, The Royal Military College of Canada, January 2009.

[25] J. Georgy, A. Noureldin, Z. Syed, and C. Goodall , "Nonlinear Filtering for Tightly Coupled RISS/GPS Integration," in *Proceedings of IEEE/ION PLANS 2010*, pp.1014-1021, Indian Wells/Palm Springs, California, USA, May 2010.

[26] IMU300—6DOF Inertial Measurement Unit: Crossbow Technology Inc., San Jose, CA.

[27] CarChip OBDII-Based Vehicle Data Logger and Software: Davis Instruments. http://www.davisnet.com/product_documents/drive/spec_sheets/8226_Specs_CarChipPro.pdf Accessed: August 21, 2012].

[28] J. Wilson, 2007 "Low-cost PND Dead Reckoning using Automotive Diagnostic Links," in *Proceedings of the 20th International Technical Meeting of the Satellite Division of the Institute of Navigation, (ION GNSS 2007)*, Fort Worth, Texas, USA, pp. 2066-2074.

[29] OEMV-1G. http://webone.novatel.ca/assets/Documents/Papers/OEMV1G.pdf [Accessed: August 21, 2012].

[30] HG1700 Inertial Measurement Unit: Honeywell. http://www51.honeywell.com/aero/common/documents/myaerospacecatalog-documents/Missiles-Munitions/HG1700_Inertial_Measurement_Unit.pdf [Accessed: August 21, 2012].

[31] OEM4-G2. http://www.novatel.ca/Documents/Papers/oem4g2.pdf [Accessed: August 21, 2012].

[32] SPAN Technology System User Manual OM-20000062: NovAtel Inc. www.novatel.com/Documents/Manuals/om-20000062.pdf [Accessed: August 21, 2012].